SDC
OPEN

FUNDUS-WIDE SUBRETINAL AND PIGMENT EPITHELIAL ABNORMALITIES IN MACULAR TELANGIECTASIA TYPE 2

MICHAEL B. POWNER, PHD,*† SASHA M. WOODS, PHD,* MEIDONG ZHU, PHD,‡§
MARK C. GILLIES, PHD,‡ PAUL S. BERNSTEIN, PHD,¶ GREGORY S. HAGEMAN, PHD,**
GRANT M. COMER, MD, MS,†† CATHERINE EGAN, MD,‡‡ MARCUS FRUTTIGER, PHD*

Purpose: Macular telangiectasia Type 2 (MacTel) causes glial and photoreceptor cell death in a small, oval patch in the central retina. Beyond this oval area, no disease manifestations have been described so far. Here, we describe a novel pathological aspect of MacTel in the retinal pigment epithelium (RPE) that is not restricted to the clinically affected area but covers the entire retina.

Methods: We have studied postmortem eyes from four patients with MacTel by immunohistochemistry and electron microscopy.

Results: We found cellular debris in the subretinal space (between photoreceptor outer segments and RPE), consisting mainly of outer segments and RPE components. In healthy eyes, the RPE normally phagocytoses the tips of the continuously growing outer segments, a process considered to be essential for photoreceptor survival. However, in the patients with MacTel, we found no evidence of ongoing outer segment phagocytosis, and the apical surface of the RPE appeared abnormal throughout most of the retina.

Conclusion: Reduced outer segment phagocytosis may explain the accumulating debris in the subretinal space but is a surprising finding because visual function in the peripheral retina is normal in patients with MacTel. Nevertheless, the subclinical pathology might induce a specific stress to which the central area is uniquely susceptible.

RETINA 0:1–9, 2017

Macular telangiectasia Type 2 (MacTel) is an uncommon eye disease causing central vision loss. Clinical manifestations of the disease include macular pigment loss, vascular changes, cavitations in the inner and outer retina, and perifoveal photoreceptor degeneration.[1] Some of the earliest signs of the disease are loss of retinal transparency[2] and loss of macular pigment in a sharply delineated, oval region in the macula,[3] which is accompanied by increased blue-light reflectance in the same oval region.[4] Importantly, all other clinical signs that have so far been described are contained within that oval region. Retinal vessels appear tortuous with hyperfluorescence in fluorescein angiography in a region that is slightly smaller than the oval area of macular pigment loss.[1,5] Also, cysts in the inner and outer retina and focal photoreceptor loss have so far only been described within that oval region.[5,6] Furthermore, postmortem histology on two patients has shown a loss of Müller cells that also matches the oval region of retinal pigment loss.[7,8] So far, no MacTel pathologies have been described outside the central area where macular pigment and Müller cell loss occurs. Although it was recently shown that MacTel patients have reduced glycine/serine levels in their serum, implicating also systemic abnormalities beyond the retinal phenotype.[9]

A previous histological study on a single case has shown evidence of substantial subretinal cellular debris in the central retina,[10] but in this study, the precise location of the pathology was not established and it is not clear how far into the retinal periphery this abnormality may be found. We have, therefore, studied postmortem eyes from four patients with MacTel, to establish the location of possible abnormalities in the entire subretinal space in MacTel and to characterize the molecular and cellular nature of these abnormalities. Furthermore, because retinal pigment epithelium (RPE) cells phagocytose the distal tips of the continuously growing photoreceptor outer segments,[11] the presence of subretinal debris can be indicative of disturbed photoreceptor outer segments phagocytosis. We, therefore, also quantified histological evidence of ongoing photoreceptor outer segment phagocytosis in the RPE by

immunohistochemistry and electron microscopy and found a strong reduction in patients with MacTel.

Methods

Clinical Imaging

Optical coherence tomography images were obtained using a spectral domain optical coherence tomography system (Spectralis OCT; Heidelberg Engineering, Heidelberg, Germany). In each case, volume scans centered on the optic nerve were obtained. Eighteen eyes from 10 patients with MacTel were analyzed.

Donors

Institutional review board/ethic committee approvals for the review of these patients' records and the analysis of the postmortem eye tissue have been obtained at the involved institutions. Details about the MacTel and anonymous control donors are summarized in Table 1. Furthermore, two previous case reports describe the characteristic clinical and histological MacTel phenotypes for MacTel Donor 1[7] and MacTel Donor 2.[8] Clinical imaging data (fluorescein angiogram and optical coherence tomography [OCT]) from MacTel Donors 3 and 4 confirm the MacTel diagnosis (see **Figure 1, Supplement Digital Content 1**, http://links.lww.com/IAE/A717). Histologically, they both displayed Müller cell loss in the central macula, similar to MacTel Donors 1 and 2 (not shown).

Tissue Processing

From each donor, the posterior pole of one eye was immersion fixed in 4% paraformaldehyde and processed as described previously (Powner et al 2010, 2013). In brief, a region that included the optic disk and fovea was embedded in wax, naso-temporal sections were cut at 6 μm and mounted onto Superfrost plus slides (VWR International LLC, Radnor, PA). Sections were deparaffinized with xylene, rehydrated through graded alcohols, and processed for immunohistochemistry. Mid peripheral samples from the other eye were placed into Karnovsky's fixative and processed for transmission electron microscopy.

Immunohistochemistry

Antigen retrieval was performed by heating the slides to 125°C in 90% glycerol (molecular grade) and 10% of 0.01 molar citrate buffer (pH 6.0) for 20 minutes. Sections were then briefly washed in water and incubated for 1 hour at room temperature in blocking buffer (1% bovine serum albumin, 0.5% triton X-100 in phosphate-buffered saline, PBS) and then in primary antibody (diluted 1:200 in blocking buffer) at room temperature for 1 hour or overnight at 4°C. Primary antibodies used were vimentin-Cy3 (C9080; Sigma-Aldrich, St. Louis, MO), retinaldehyde-binding protein 1 (RLBP1) (MA1-813, Pierce Antibodies; Thermo Fisher Scientific Inc, Waltham, MA), rhodopsin (MAB5356; Millipore, Billerica, MA), M-L opsin (AB5405; Millipore), zona occludens 1 (ZO-1) (Invitrogen, Paisley, United Kingdom), MER proto-oncogene, tyrosine kinase (MERTK) (ab52968; Abcam, Cambridge, United Kingdom), Stimulated By Retinoic Acid 6 (Stra6) (ab73490; Abcam), and RPE65 (MAB5428; Millipore). Sections were washed in washing buffer (0.1% Tween20 in PBS) and incubated for 1 hour at room temperature in secondary antibodies (Invitrogen, diluted 1:200 in blocking buffer). Subsequently, sections were washed in PBS, treated with Hoechst (10 μg/mL in PBS) for 30 seconds, washed again in PBS, and mounted in Mowiol mounting medium (Sigma). Images were taken using a Leica (Wetzlar, Germany) DM IRB fluorescent microscope or a Zeiss (Oberkochen, Germany) LSM700 confocal microscope.

Electron Microscopy

Karnovsky's fixed tissue was osmium tetroxide–treated, dehydrated, and embedded in araldite resin.

From the *MacTel Research Group, UCL Institute of Ophthalmology, University College London, London, United Kingdom; †Applied Vision Research Centre, School of Health Sciences, City University London, London, United Kingdom; ‡Save Sight Institute, University of Sydney, Sydney, Australia; §Lions New South Wales Eye Bank, Sydney Eye Hospital, New South Wales Organ and Tissue Donation Service, Sydney, Australia; ¶Department of Ophthalmology and Visual Sciences, School of Medicine, Moran Eye Center, University of Utah, Salt Lake City, Utah; **Department of Ophthalmology and Visual Sciences, Sharon Eccles Steele Center for Macular Degeneration, John A. Moran Eye Center, University of Utah, Salt Lake City, Utah; ††W.K. Kellogg Eye Center, University of Michigan, Ann Arbor, Michigan; and ‡‡MacTel Research Group, Moorfields Eye Hospital NHS Foundation Trust, London, United Kingdom.

Supported by The Lowy Medical Research Institute.

None of the authors has any financial/conflicting interests to disclose.

M. B. Powner conducted experiments. M. Zhu, M. C. Gillies, P. S. Bernstein, G. S. Hageman, and G. M. Comer collected and processed tissue and clinical information from donors. M. B. Powner and S. M. Woods analyzed data and prepared figures. M. B. Powner, S. M. Woods, M. Fruttiger, and C. Egan conceived experiments and wrote the manuscript.

Supplemental digital content is available for this article. Direct URL citations appear in the printed text and are provided in the HTML and PDF versions of this article on the journal's Web site (www.retinajournal.com).

Reprint requests: Marcus Fruttiger, PhD, UCL Institute of Ophthalmology, University College London, 11-43 Bath Street, London EC1V 9EL, United Kingdom; e-mail: m.fruttiger@ucl.ac.uk

Table 1. Summary of Donor Details

No.	Sex	Age	Diagnosis*	Comorbidities	Cause of Death	Postmortem Delay, Hours†
MacTel donors						
1[7]	M	65	54	Type 2 diabetes	Cardiovascular accident	4
2[8]	F	61	52	Scleroderma	Respiratory failure	3.5
3	F	49	46		Uterine leiomyosarcoma	2.5
4	M	78	69	Senile dementia	Myocardial infarction	18
Control donors with no reported ophthalmic pathology						
1	M	63			Lung cancer	8
2	F	66			Stroke	10
3	M	67			Cardiovascular accident	7
4	M	70			Stroke	11

*Age of patient when MacTel was diagnosed.
†Time between death and fixation of the eye.

Images of the RPE were taken using a Jeol 1,010 transmission electron microscope (Jeol, Welwyn Garden City, United Kingdom) fitted with a Gatan Orius SC1000B camera (Gatan, Abingdon, United Kingdom).

Phagosome Counts

Electron microscopy: From each donor (control and MacTel), the number of phagosomes present within 260 RPE cells (cells analyzed with visible nuclei) was counted manually. Immunohistochemistry: The number of opsin-positive outer segments was counted within 3,000 RPE cells on sections stained for ml-opsin and rhodopsin. The number of RPE cells was determined by the number of Hoechst-positive nuclei. Stained phagosomes had to be present below the apical surface of the RPE (determined using differential interference contrast microscopy) to be counted. Student's *t*-test was used for statistical analysis.

Results

Debris in MacTel Type 2 Eyes Spans the Entire Retina and Consists of Retinal Pigment Epithelium, Glial, and Pneumatic Retinopexy Components

In an initial effort to establish the location and frequency of possible subretinal abnormalities in patients with MacTel, we investigated this phenotype clinically using OCT. In 5 of 18 eyes examined (10 patients), we found small hyperreflective patches in the subretinal space. Figure 1, A and B show exemplary OCT scans from a MacTel patient with such anomalies. However, because of the limited resolution of these scans, it is difficult to further characterize the precise nature and location of the observed hyperreflective patches, and we used histological analysis on postmortem eyes from four different MacTel donor eyes, all of which manifested typical loss of Müller cells in the centre of the macula (not shown). This revealed in all four eyes small clumps of debris between photoreceptor outer segments and the RPE (arrows in Figure 1, C–H). Interestingly, the debris did not present uniformly in all four eyes—Donor 2 showed large deposits across the entire peripheral retina, including the macula, whereas in the other three donors, the debris clumps were only found near the optic nerve head. All debris clumps were devoid of nuclei and contained melanin granules (Figure 1, G and H).

We next sought to establish the cellular origin and molecular nature of the subretinal debris clumps. The presence of melanin granules suggests a contribution from RPE cells—the apical processes of which contain melanin. Positive immunohistochemistry staining for retinaldehyde-binding protein 1 (RLBP1, also known as CRALBP)—a protein involved in the regeneration of visual pigment and a well-known marker of RPE cells—indicated that these clumps of debris contain RPE components (Figure 2, A and B). Some patches also contained vimentin-positive and glial fibrillary acidic protein–positive structures (Figure 2C), which might be derived from Müller cells or astrocytes.

Because a previous examination of subretinal debris in a patient with MacTel using electron microscopy showed an accumulation of degenerate photoreceptor elements,[10] we used antibodies specific for medium and long-wavelength opsin (ml-opsin) and rhodopsin to visualize photoreceptor outer segments in all four donor eyes and found positive staining in all subretinal debris clumps (Figure 2, D and E). However, staining for COX2 (a marker of mitochondria, which are highly represented in the inner segments) was negative (Figure 2F). Furthermore, despite the accumulation of RPE, glial, and photoreceptor components, there seemed to be no immune response in the subretinal space, as $CD16^+$ cells were only present in the inner retina, and not in the clumps of debris (Figure 2, G and H).

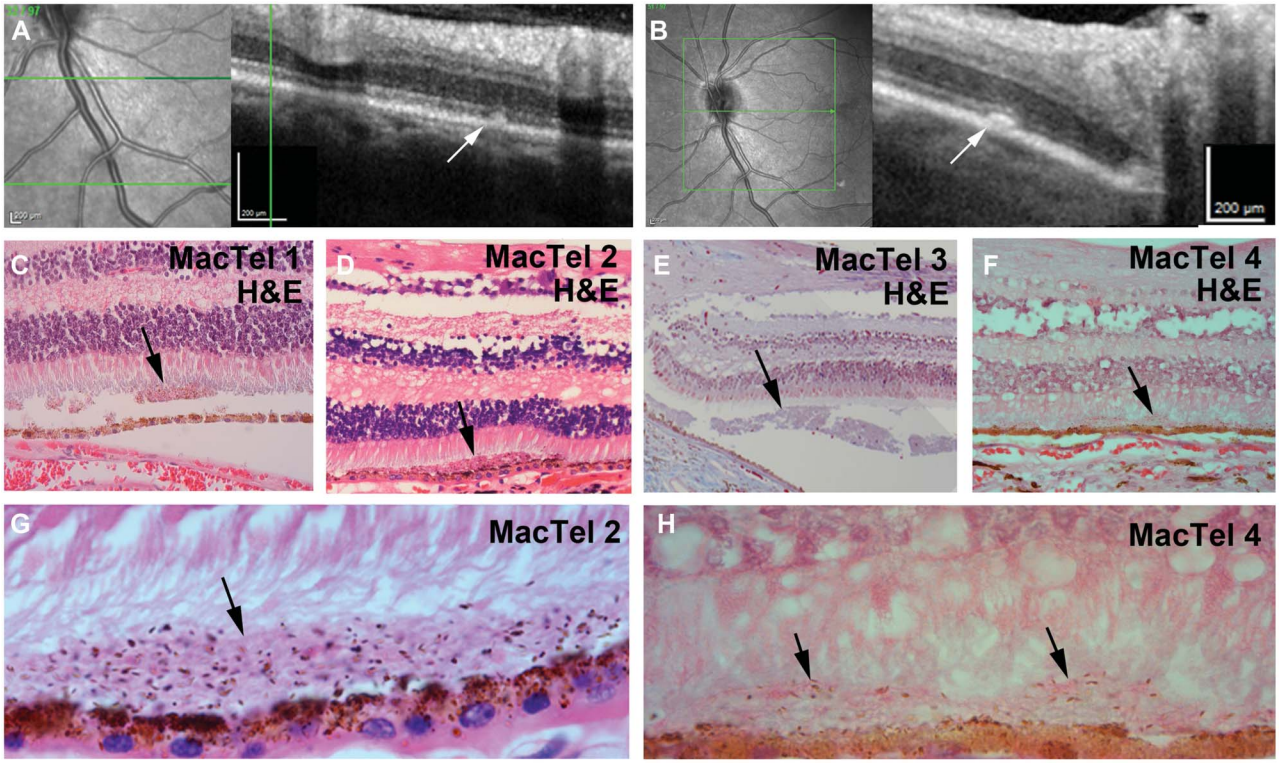

Fig. 1. Subretinal deposits in patients with MacTel. **A** and **B.** Examples of subretinal patches (arrows) seen by OCT in a patients with MacTel. **C–F.** Hematoxylin and eosin (H&E) stained sections of four postmortem donor eyes from four different patients with MacTel. Debris clumps (arrows) situated between the photoreceptors and the RPE were found in proximity to the optic nerve in all four donor eyes. **G** and **H.** Higher magnification shows pigment granules in the debris clumps.

The Apical Surface of MacTel Type 2 Retinal Pigment Epithelium Is Structurally Abnormal

Having established the cellular composition of the subretinal debris clumps, we next examined the ultrastructure of the debris and RPE. This revealed a thin layer of material on the apical surface of the RPE throughout most of the retina in the patients with MacTel, which is not found in controls (Figure 3, A and B). This thin layer was found independently of the larger debris clumps described and covered a much larger area. Strikingly, direct physical interactions between photoreceptor outer segments and RPE appear to be precluded by the thin deposit. The thin debris layer contained outer segment fragments and large membrane bound vesicles (Figure 3, C and D). It is possible that the round vesicle-like structures are derived from degenerating rod outer segments because we observed a continuum of intermediate stages between these two structures (Figure 3, E–H). In the specimen with the shortest postmortem delay before fixation, we also found smaller granular structures—possibly tubule in nature (Figure 3, I–K). In terms of size, they are consistent with apical RPE processes. However, the apical surface of RPE cells in patients with MacTel is largely devoid of apical processes (Figure 3, L and M), and in locations where they could be found, they had a very unusual, thickened appearance (Figure 3, N and O).

The Retinal Pigment Epithelium Is Normally Polarized in MacTel Type 2

Because the apical surface of the RPE was shown to be abnormal in MacTel Type 2 eyes, we next asked if the RPE is abnormally polarized (Figure 4). Retinal pigment epithelium–specific 65 kDa protein (RPE65) showed normal cytosolic distribution, whereas Stimulated by retinoic acid 6 (STRA6) and Cytokeratin 8 (CK8) were both normally expressed on basal and junctional surfaces (Figure 4, A–C). Similarly, tight junction protein 1 (ZO1) was also correctly located near the apical surface of the RPE (Figure 4D). These findings suggest that the RPE is indeed normally polarized, despite the abnormal morphology of the apical surface.

However, we noticed a reduced expression of tyrosine-protein kinase Mer (MERTK) in the RPE of patients with MacTel compared with controls. Normally, MERTK—a protein which plays an important role in the phagocytic uptake of photoreceptor outer segments by the RPE—is strongly expressed on the

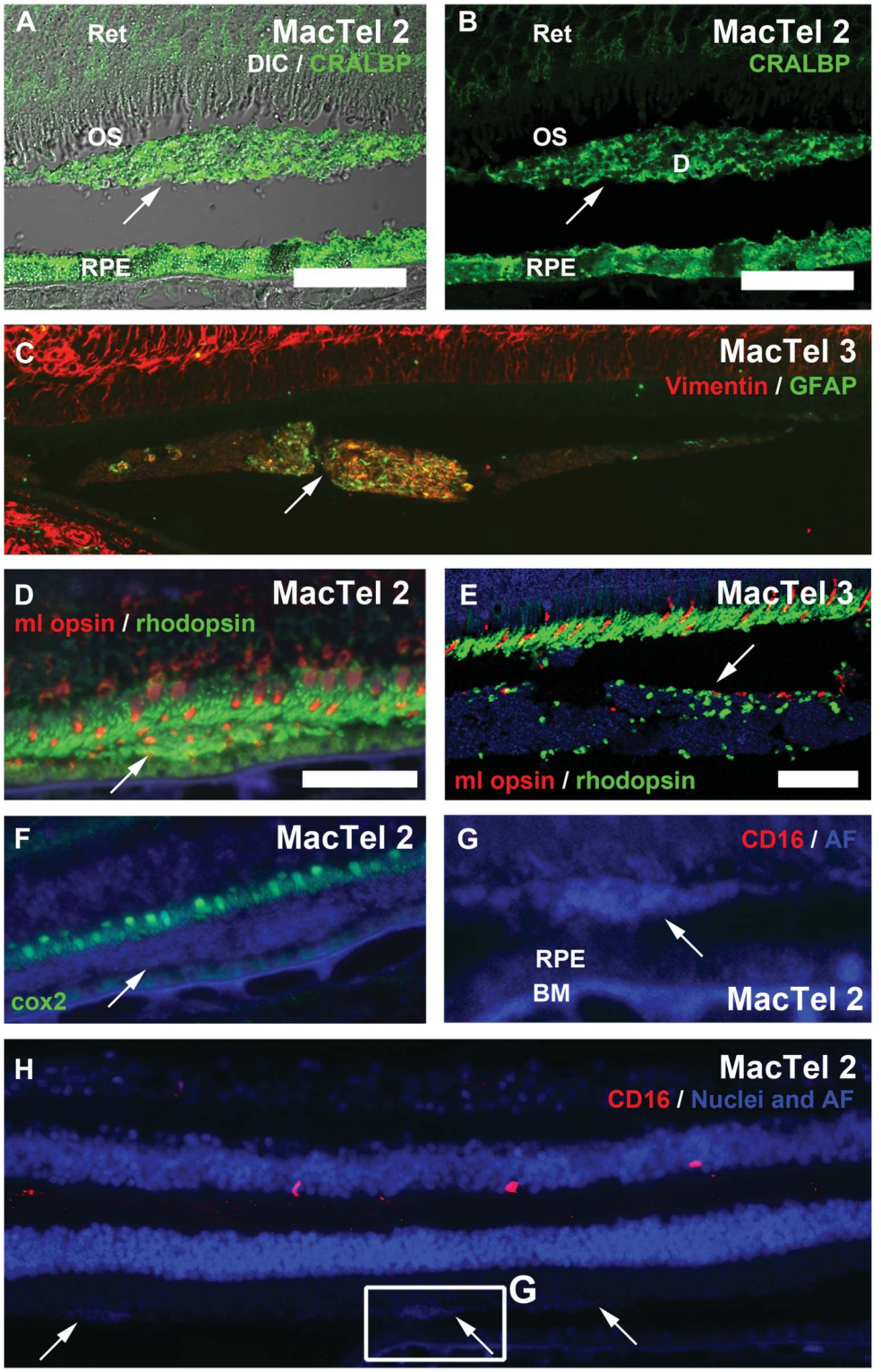

Fig. 2. Molecular characterization of subretinal debris clumps in MacTel eyes. **A** and **B.** CRALBP-positive structures were found in all debris clumps from all four postmortem MacTel donor eyes. **C.** Vimentin (red) and glial fibrillary acidic protein (green) was also detected in some regions in the eyes of Donors 1 and 3, suggestive of glial components. **D** and **E.** ML-opsin (red) and rhodopsin (green) staining was detected in all clumps in all four donor eyes, indicating the presence of photoreceptor outer segments. **F.** The absence of COX2 (a mitochondrial marker) in the debris clumps suggests an absence of photoreceptor inner segments. **G** and **H.** CD16-positive cells were only found in the retina, but not in the debris clumps, suggesting that there is no immune response in the subretinal space. Arrows indicate subretinal debris clumps. BM, basement membrane; D, debris; OS, outer segment; Ret, Retina. Scale bars 50 μm.

apical surface of the RPE (Figure 4E). However, in the MacTel samples, MERTK was only very weakly expressed at the apical surface of the RPE and was also detected within the subretinal debris clumps (Figure 4, F and G).

Lack of Histological Evidence for Outer Segment Phagocytosis

The reduced MERTK expression and the abnormal apical surface of the RPE are indicative of a potential decrease of outer segment phagocytosis by the RPE.

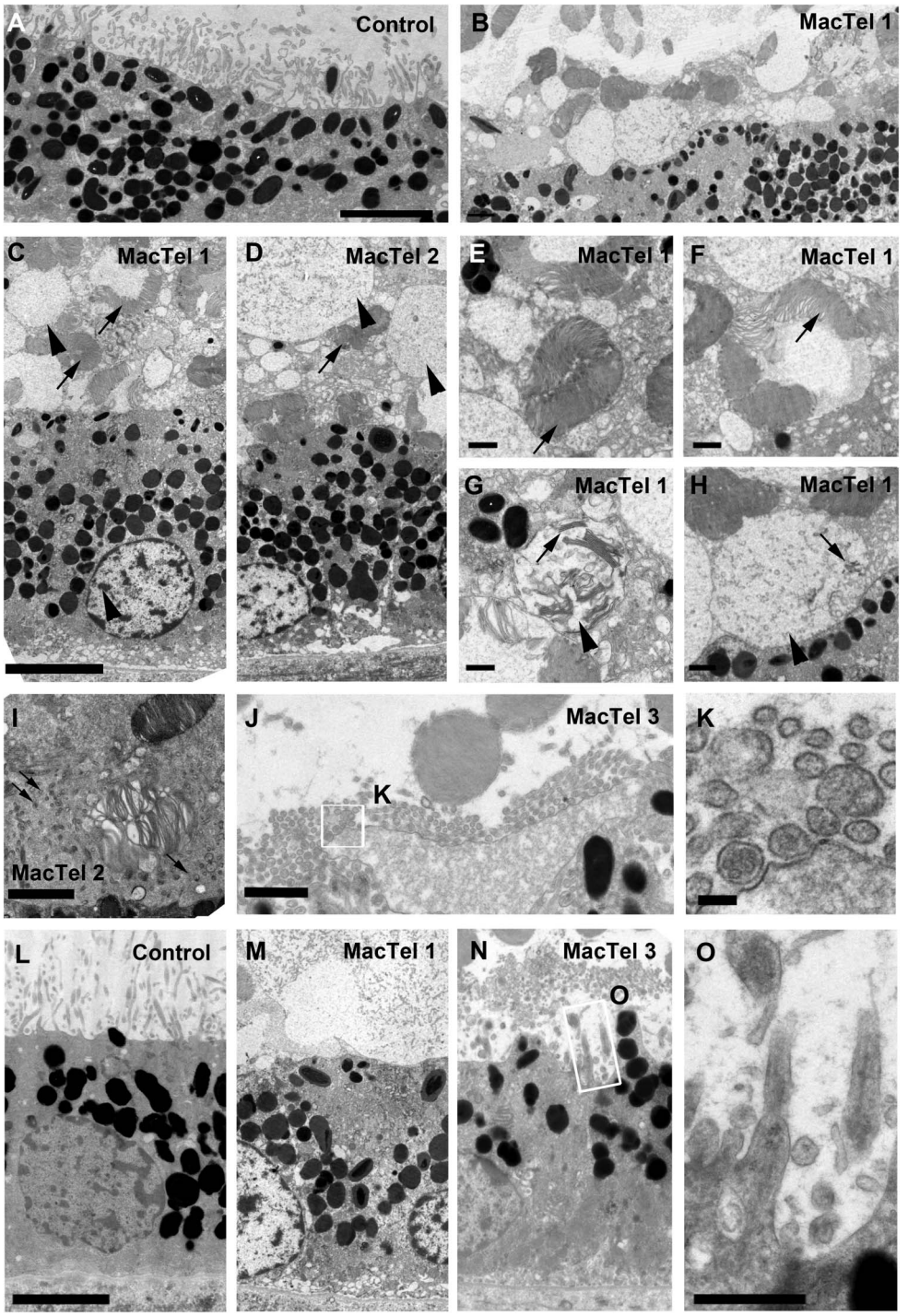

Fig. 3. Ultrastructural analysis reveals debris layer on apical RPE surface. **A.** In healthy control tissue, the RPE displays processes at the apical surface. **B.** By contrast, a thin layer of debris sits on the apical surface of the RPE in patients with MacTel. **C** and **D.** The debris layer consist of outer segment fragments (arrows) and large round vesicle-like structures (arrowheads). **E–H.** At a morphological level, intermediates between the degenerating outer segments (arrows) and the round vesicles (arrowheads) can be found, with some round vesicles containing fragments of degenerating disks. **I–K.** Small spherules could also be found, which based on size, might be related to degenerating apical processes of the RPE. **L** and **M.** Apical processes, normally seen in healthy RPE, are largely absent in MacTel tissue. **N** and **O.** In places where some apical processes could be found, they appear abnormally thick and distorted. Scale bar in **A–D**: 5 μm; **E–H**: 0.5 μm; **I**: 2 μm; **J**: 1 μm; **K**: 150 nm; **L–N**: 5 μm; **O**: 150 nm.

Because it is not possible to measure this function of the RPE directly, we used as an indirect readout the presence of ingested outer segments within the RPE cells. We used immunohistochemistry staining for ml-opsin and rhodopsin to visualize internalized but not yet fully digested outer segments. In control eyes from four different donors, we frequently found ml-opsin or rhodopsin-positive dots within RPE cells (Figure 5, A–D), whereas in the four MacTel samples, the positively stained dots were almost exclusively located at the apical surface of the RPE cells. Quantification revealed a highly significant difference between the controls and the patients with MacTel (Figure 5, I and J). As an alternative method to assess the number of ingested outer segments, we also used electron microscopy to identify RPE phagosomes, which can be easily identified by this method in

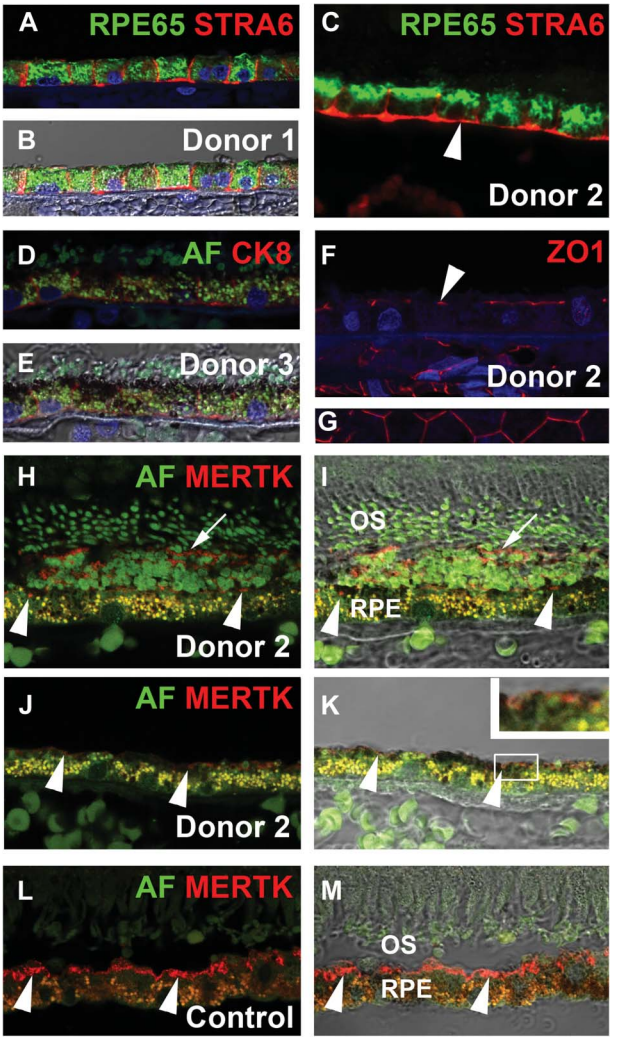

Fig. 4. The RPE is polarized normally in MacTel retina. **A–C.** RPE65 staining (green) shows normal cytosolic distribution, whilst STRA6 (red) shows normal basal and junctional localization in patients with MacTel. **D** and **E.** CK8 (red) is also expressed normally within basal and junctional surfaces. Autofluorescence (green) shows lipofuscin which appears yellow. **F** and **G.** The apical marker ZO1 is also normally localized in junctions near the apical surface, which are continuous. **H–K.** In patients with MacTel, MERTK (red) is found in debris clumps (arrows) and only weakly expressed on the apical RPE surface (arrowheads). **L** and **M.** In contrast, in control retina, MERTK is strongly expressed at the apical surface (arrowheads). AF, autofluorescence; CK8, cytokeratin 8; OS, outer segments; DIC, differential interference contrast microscopy.

control patients (Figure 5, K–M). In the MacTel samples, phagosomes could only rarely be found (Figure 5N) and were drastically reduced in numbers (Figure 5O).

Discussion

We have studied four MacTel Type 2 postmortem eyes (from four different patients) and found in all of them subretinal debris, ultrastructural abnormalities in the RPE, and reduced outer segment phagosomes throughout the retina. These findings are remarkable for two reasons. First, we found these abnormalities in the peripheral and in the central retina, which makes this the first report of a MacTel Type 2 pathology outside the clinically affected, central retina. However, the abnormalities we found appear to be at the threshold of clinical detection because so far neither functional deficits nor structural abnormalities have been described in the peripheral retina of living patients with MacTel Type 2. A previous report described a build-up of subretinal material in the foveal region in some patients,[10] but this phenotype did not affect the periphery. Furthermore, none of our four postmortem samples fell into that category. Nevertheless, we cannot entirely exclude the possibility that our histological analysis has been affected by artefactual postmortem changes. Further clinical imaging studies, using high resolution OCT should therefore be performed to confirm the presence of subretinal debris in living patients with MacTel.

The second remarkable finding in our study is the lack of evidence for outer segment phagocytosis in the presence of apparent normal peripheral retinal function. Defects in this process are usually linked to more severe phenotypes, such as photoreceptor cell death. For instance, Royal College of Surgeon (RCS) retinal dystrophic rats display debris build-up in the subretinal space and photoreceptor degeneration within 2 weeks to 3 weeks after birth.[12] In these animals, RPE cells are unable to phagocytose photoreceptor outer segments[13] because of a mutation in the receptor tyrosine kinase gene *Mertk*.[14] Similarly, mutations in the human orthologue (*MERTK*) can cause retinitis pigmentosa, an inherited eye disease with progressive rod degeneration.[15] Furthermore, defects in cell internal phagosome processing are linked to Usher Type 1B syndrome, a congenital disorder with progressive loss of hearing and vision.[16] In light of this, it may appear surprising that peripheral photoreceptors are not affected in MacTel, despite the severe RPE abnormalities in the peripheral retina in our tissue donors.

However, how exactly defects in outer segment phagocytosis can cause pneumatic retinopexy degeneration is likely to be disease and context dependent. In age-related macular degeneration, for instance, it has been suggested that inefficient outer segment phagocytosis may cause a build-up of photo-oxidized products or other toxic by-products, leading to RPE cell death and photoreceptor degeneration.[17] In some patients with age-related macular degeneration, subretinal deposits have been described,[18,19] although the nature of the subretinal material in these studies appears to be different from what we found in our MacTel samples. However, in adult foveomacular vitelliform dystrophy, at

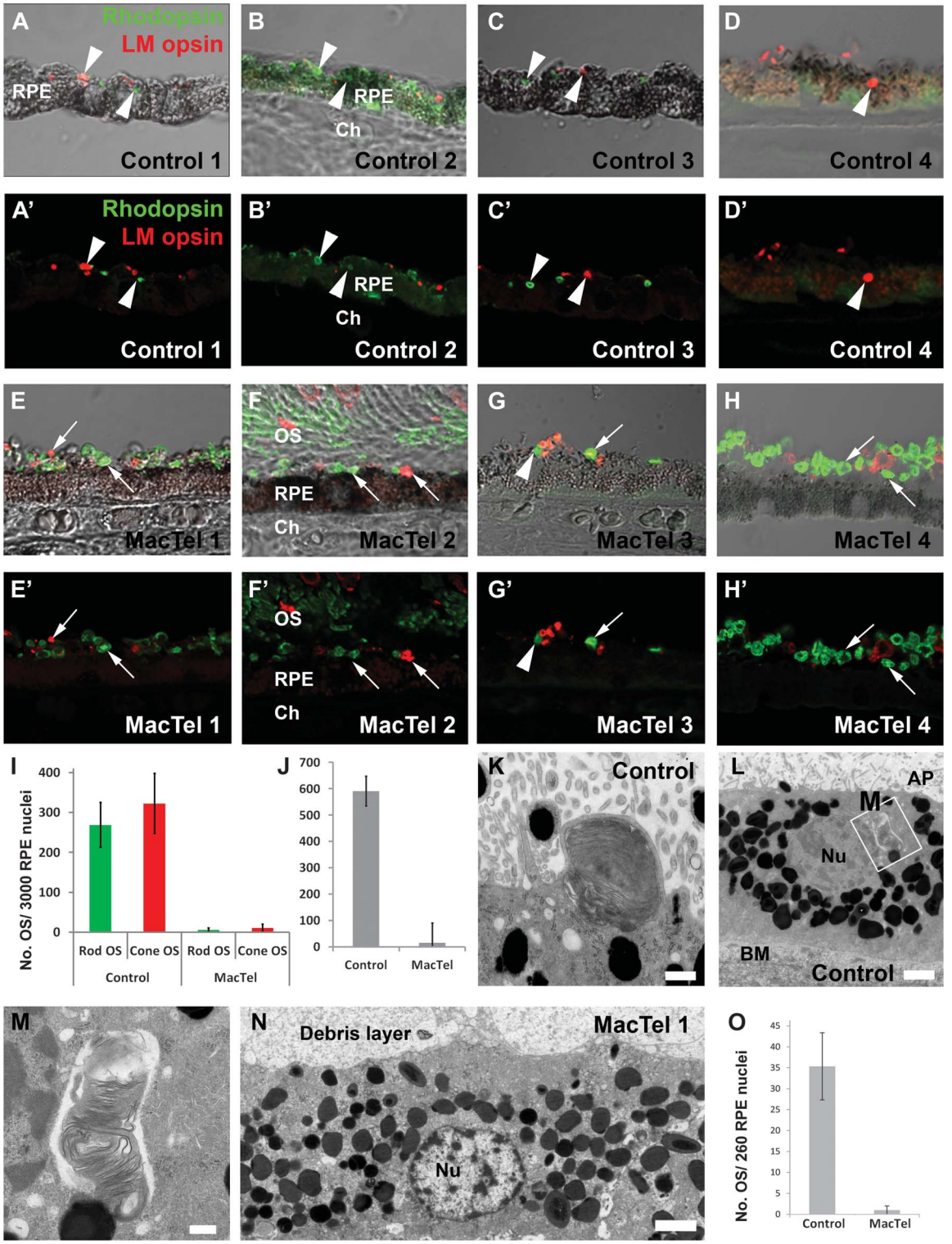

Fig. 5. Reduced outer segment phagocytosis in MacTel. **A–D.** In control eyes, rhodopsin and LM-opsin positive outer segments can be found within RPE cells (arrowheads). **E–H.** By contrast, there are almost no outer segments within the RPE of patients with MacTel, with outer segments only visible on the apical surface of the RPE (arrows). **I** and **J.** Quantification of immunohistochemistry based localization of rod and cone outer segments from four control and four patients with MacTel shows a strong reduction of internalized outer segments in patients with MacTel (rods: $P = 0.020$, cones: $P = 0.038$, total: $P = 0.029$). **K–N.** Outer segment phagocytosis can also be assessed by electron microscopy, as outer segments are capture at the apical RPE surface (**K**) and then internalized in phagosomes (**L** and **M**). In patients with MacTel, phagosomes were rarely observed (**N**) and quantification of four control and four patients with MacTel showed a dramatic reduction in the patients with MacTel (**O**). Ch, choroid; OS, outer segment; AP, apical processes; Nu, nucleus; BM, Bruch's membrane; Scale bars are **K**: 0.5 μm, **L**: 2 μm, **M**: 0.4 μm, **N**: 2 μm.

least during the early stages, photoreceptors maintain good function, despite a thick layer of debris obstructing direct access to the RPE.[20,21] This makes normal phagocytosis difficult to imagine in patients with adult foveomacular vitelliform dystrophy and demonstrates that loss of outer segment phagocytosis does not necessarily lead to photoreceptor degeneration. It is possible that macrophages take over some of the phagocytic load in such situations, but we have not found any evidence for increased subretinal macrophage numbers in our MacTel samples.

The fact that subretinal abnormalities were found in all four patients with MacTel so far analyzed by histology, suggests that this subclinical phenotype may be common in patients with MacTel. Whether it occurs in all patients with MacTel is not known. Furthermore, unlike the very specific loss of Müller cells in a specific region in the macula,[7,8] the phenotype described in this study does not appear to be MacTel specific. We commented previously on similarities between MacTel and adult foveomacular vitelliform dystrophy.[10] In both diseases, degrading outer segments appear in the subretinal space, covering the apical surface of the RPE. But whether the subretinal debris in MacTel is a consequence or a cause of reduced phagocytosis by the RPE is not clear. It is also possible that altered photoreceptors can lead to reduced phagocytosis. For instance, the composition of different phospholipids in the outer segment plasma membrane can influence outer segment phagocytosis by the RPE.[22] Thus, it is possible that a general dysfunction in photoreceptor or RPE physiology can contribute to the pathobiology in MacTel by introducing a stress, which might be tolerated in the periphery but not in the macula.

Key words: MacTel, photoreceptors, outer segment phagocytosis, RPE.

Acknowledgments

The authors are also grateful to Moorfields Eye Bank and UCL Biobank, and the National Institute for Health Research (NIHR) Biomedical Research Centre at Moorfields Eye Hospital NHS Foundation Trust and UCL Institute of Ophthalmology for support in this project.

References

1. Charbel Issa P, Gillies MC, Chew EY, et al. Macular telangiectasia type 2. Prog Retin Eye Res 2013;34:49–77.
2. Gass JD, Blodi BA. Idiopathic juxtafoveolar retinal telangiectasis. Update of classification and follow-up study. Ophthalmology 1993;100:1536–1546.
3. Issa Charbel P, Berendschot TTJM, Staurenghi G, et al. Confocal blue reflectance imaging in type 2 idiopathic macular telangiectasia. Investig Ophthalmol Vis Sci 2008;49: 1172–1177.
4. Sallo FB, Leung I, Zeimer M, et al. Abnormal retinal reflectivity to short-wavelength light in type 2 idiopathic macular telangiectasia. Retina 2017. doi: 10.1097/IAE. 0000000000001728.
5. Sallo FB, Leung I, Clemons TE, et al. Multimodal imaging in type 2 idiopathic macular telangiectasia. Retina 2015;35:742–749.
6. Barthelmes D, Gillies MC, Sutter FKP. Quantitative OCT analysis of idiopathic perifoveal telangiectasia. Invest Ophthalmol Vis Sci 2008;49:2156–2162.
7. Powner MB, Gillies MC, Tretiach M, et al. Perifoveal Müller cell depletion in a case of macular telangiectasia type 2. Ophthalmology 2010;117:2407–2416.
8. Powner MB, Gillies MC, Zhu M, et al. Loss of Müller's cells and photoreceptors in macular telangiectasia type 2. Ophthalmology 2013;120:2344–2352.
9. Scerri TS, Quaglieri A, Cai C, et al. Genome-wide analyses identify common variants associated with macular telangiectasia type 2. Nat Genet 2017;49:559–567.
10. Cherepanoff S, Killingsworth M, Zhu M, et al. Ultrastructural and clinical evidence of subretinal debris accumulation in type 2 macular telangiectasia. Br J Ophthalmol 2012;96:1404–1409.
11. Kevany BM, Palczewski K. Phagocytosis of retinal rod and cone photoreceptors. Physiology (Bethesda) 2010;25:8–15.
12. Dowling JE, Sidman RL. Inherited retinal dystrophy in the rat. J Cell Biol 1962;14:73–109.
13. Edwards RB, Szamier RB. Defective phagocytosis of isolated rod outer segments by RCS rat retinal pigment epithelium in culture. Science 1977;197:1001–1003.
14. D'Cruz PM, Yasumura D, Weir J, et al. Mutation of the receptor tyrosine kinase gene Mertk in the retinal dystrophic RCS rat. Hum Mol Genet 2000;9:645–651.
15. Gal A, Li Y, Thompson DA, et al. Mutations in MERTK, the human orthologue of the RCS rat retinal dystrophy gene, cause retinitis pigmentosa. Nat Genet 2000;26:270–271.
16. Gibbs D, Kitamoto J, Williams DS. Abnormal phagocytosis by retinal pigmented epithelium that lacks myosin VIIa, the Usher syndrome 1B protein. Proc Natl Acad Sci U S A 2003;100: 6481–6486.
17. Terman A, Brunk UT. Lipofuscin. Int J Biochem Cell Biol 2004;36:1400–1404.
18. Curcio CA, Messinger JD, Sloan KR, et al. Subretinal drusenoid deposits in non-neovascular age-related macular degeneration: morphology, prevalence, topography, and biogenesis model. Retina 2013;33:265–276.
19. Greferath U, Guymer RH, Vessey KA, et al. Correlation of histologic features with in vivo imaging of reticular pseudodrusen. Ophthalmology 2016;123:1–12.
20. Arnold JJ, Sarks JP, Killingsworth MC, et al. Adult vitelliform macular degeneration: a clinicopathological study. Eye (Lond) 2003;17:717–726.
21. Chowers I, Tiosano L, Audo I, et al. Adult-onset foveomacular vitelliform dystrophy: a fresh perspective. Prog Retin Eye Res 2015;47:64–85.
22. Ryeom SW, Silverstein RL, Scotto A, Sparrow JR. Binding of anionic phospholipids to retinal pigment epithelium may be mediated by the scavenger receptor CD36. J Biol Chem 1996;271:20536–20539.